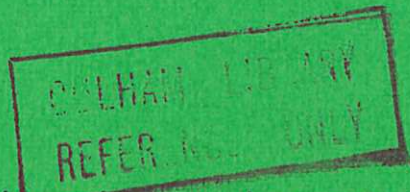




UKAEA RESEARCH GROUP

Report



An absolutely calibrated x-ray image intensifier and high-speed shutter based on a channel multiplier array for the detection of radiation from high-density plasmas.

(Joint European Programme on Plasma Focus)

M G HOBBY
J-P RAGER
N J PEACOCK



CULHAM LABORATORY
Abingdon Berkshire

1974

Available from H. M. Stationery Office

Enquiries about copyright and reproduction should be addressed to the Librarian, UKAEA, Culham Laboratory, Abingdon, Berkshire, England

U.D.C.
537.531.083
621.383.8

An absolutely calibrated x-ray image intensifier and high-speed shutter based on a channel multiplier array for the detection of radiation from high-density plasmas.

(Joint European Programme on Plasma Focus)

M. G. Hobby,* J-P. Rager[/] and N. J. Peacock

ABSTRACT

An x-ray image intensifier based on a channel multiplier array has been developed to overcome the low overall sensitivity of wavelength dispersive crystal spectrometers. A prototype instrument has been absolutely calibrated on standard x-ray sources and tested on two high-density plasmas. In addition to demonstrating a sensitivity gain of the order of 100 without appreciable loss of resolution, the intensifier has been successfully shuttered for times as short as 12 nano-seconds by pulsing the accelerating voltage on to the channel plate.

* Attached from Leicester University

[/] Laboratori Gas Ionizzati, Euratom (CNEN), Italy

UKAEA Research Group
Culham Laboratory
Abingdon
Oxon

May 1974

SBN: 85311 026 3

Introduction

One of the most pressing problems associated with high-resolution X-ray spectroscopy of short-lived, high-density plasmas such as the Plasma Focus (1, 2) and laser-produced plasmas (3, 4) is the low sensitivity of crystal dispersion instruments employing photographic recording. This often means that many discharges are needed to integrate an intense enough record, which makes interpretation less certain and effectively rules out short-exposure time-resolution of the discharge. An X-ray image intensifier based on a channel multiplier array (5) has been developed to overcome these difficulties. A prototype instrument has been constructed, calibrated on standard X-ray sources, and tested on two high-density plasma discharges as part of a collaborative study with the Plasma Focus Group of CNEN Laboratori Gas Ionizzati (Frascati). In addition to demonstrating a presentable gain in sensitivity of the order of 100 with little loss of resolution, the intensifier has been successfully shuttered for times as short as 12 nsec by pulsing the accelerating voltage on to the channel plate.

Principle, Design and Construction of the Intensifier

The principle of the intensifier system is not new (6, 7, 8), but the type of mounting used here is novel (9). The fast switching capability applied directly to the channel plate has not been reported previously, though nanosecond gating of Vidicon tubes coupled to the fibre-optic output has been demonstrated recently (10, 11). The present system is shown schematically in Figure 1 and in constructional detail in Figure 2. X-rays striking the front face of the Mullard G40-25 channel multiplier array release photoelectrons which are accelerated down the individual tubes by the primary potential V_A . These in turn strike the

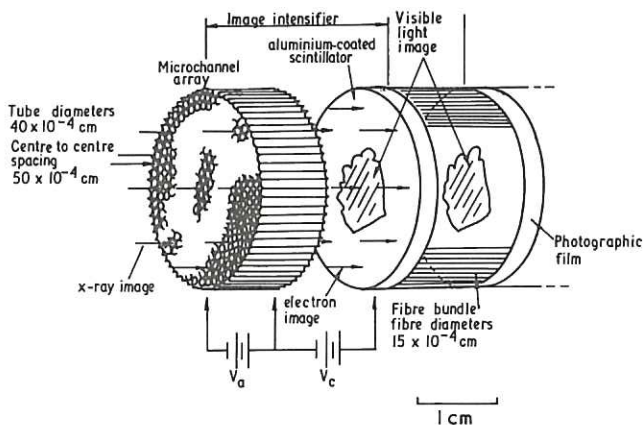


Figure 1. Schematic diagram of the channel plate X-ray image intensifier system showing the electrical and optical interfaces.

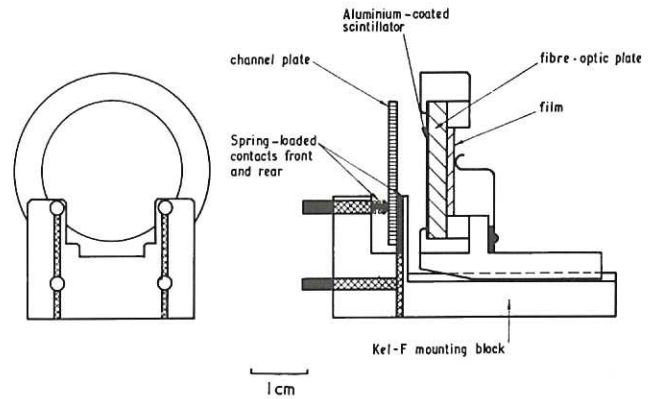


Figure 2. Constructional details of the channel plate X-ray image intensifier system.

inner walls after gaining energy and produce further secondary electrons. The total electron gain of a channel depends, among other things, on the applied voltage and is typically of the order of 10^4 at 1 kilovolt. The electrons emerging from the rear of the plate have energies of only a few tens of electron volts and are collected by applying a secondary potential, V_C , of several kilovolts, between the plate and a $5 \mu\text{m}$ thick layer of NE 102 plastic scintillator coated with 250 \AA of aluminium to provide electrical contact. The electrons traverse the aluminium and are stopped in the scintillator where the resulting proximity focussed visible image is transmitted to photographic film via a thin fibre-optic transfer plate. The scintillator is deposited on the fibre-optics by centrifugal evaporation of the scintillator in xylene.

The major practical considerations in constructing the intensifier are to ensure clean, firm electrical and mechanical contacts to the channel plate faces, to eliminate the possibility of tracking, and to maintain a high vacuum in the vicinity of the plate. The construction of the mount therefore leaves the channel plate and film holder completely open and separate from each other. This necessitates film loading under safe-light conditions and the provision of light-sealing foils between the radiation source and the intensifier but avoids having to break electrical contact at each loading. The insulating parts of the mount are made of Kel-F or P.T.F.E. which have high surface resistance and low outgassing properties. Electrical and mechanical contact is made via front and rear spring-loaded contacts at two points only. Both sets of contacts are gold-coated and mate with gold annuli evaporated on to the channel plate faces.

Monitoring Circuits and High-Voltage Supplies

The most sensitive monitor of good operating

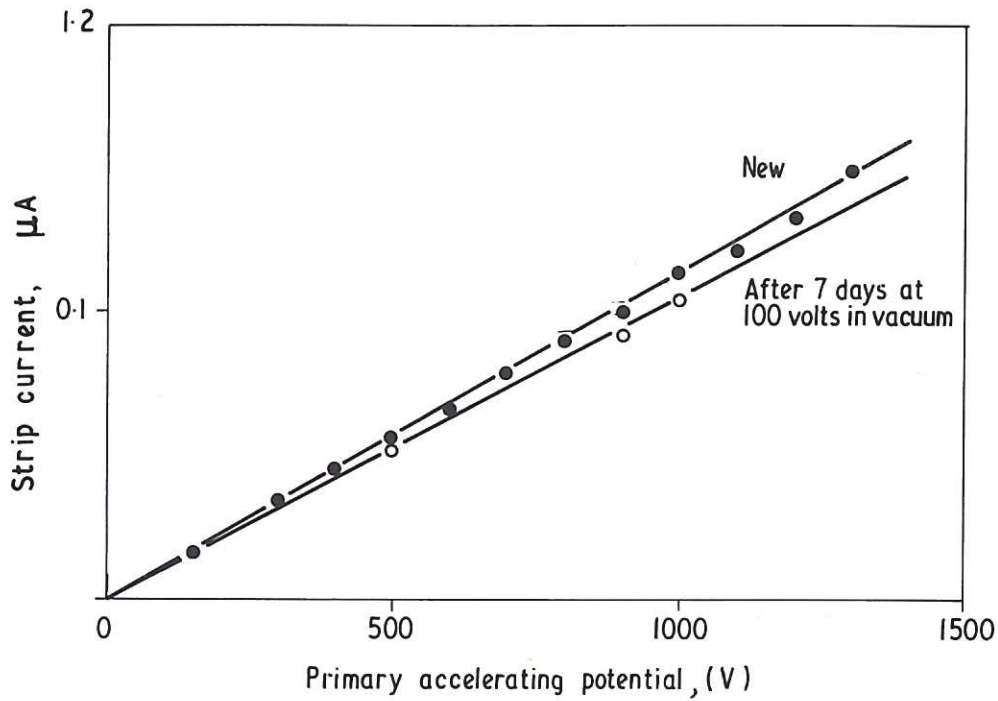


Figure 3. Strip current as a function of the primary potential for a Mullard G40-25 channel plate.

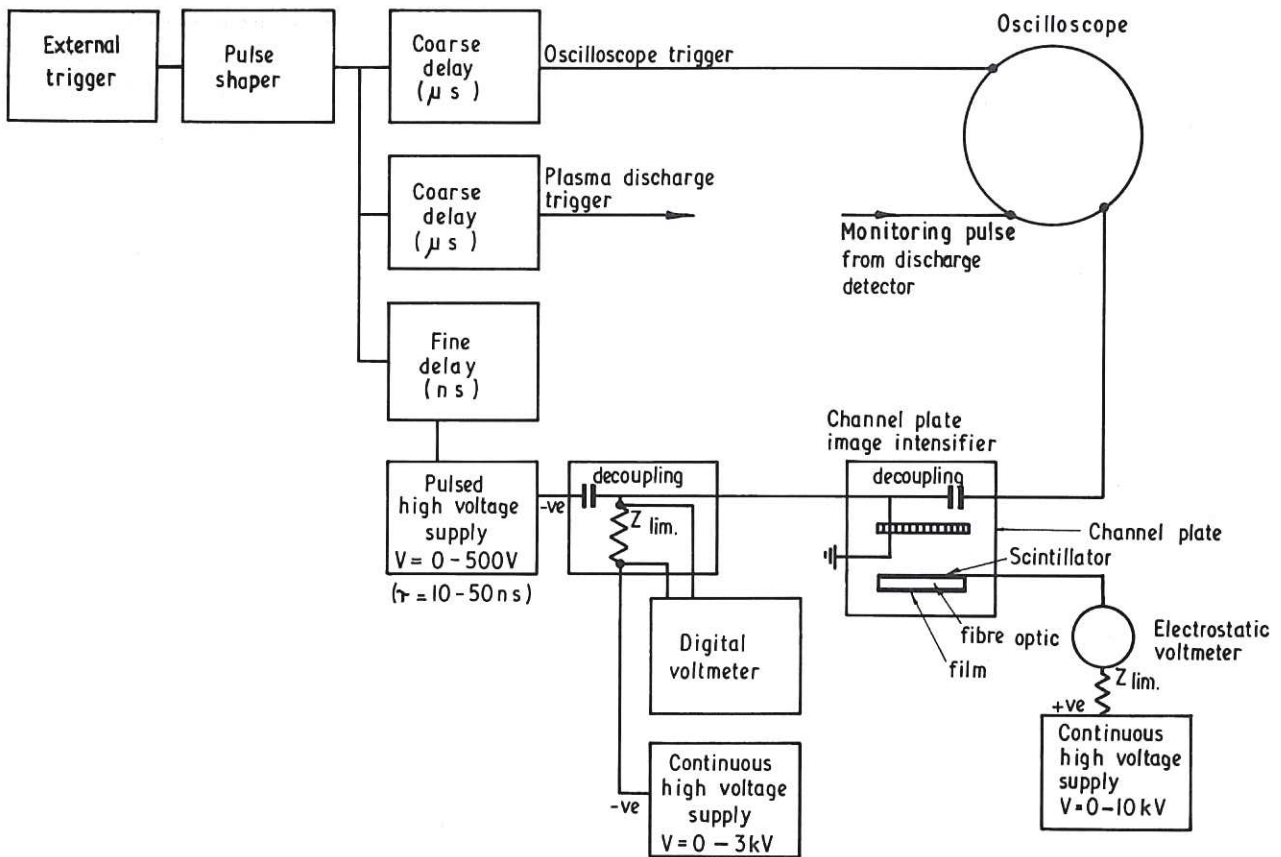


Figure 4. Schematic diagram of the essential monitoring and supply circuits to the image intensifier as it would be used in a typical experimental arrangement.

characteristics in a channel plate, i.e. good electrical contact to the plate faces, low noise level and freedom from water vapour and other contaminants, is the strip current. This is continuously recorded on a digital voltmeter as the voltage across a limiting resistor in series with the channel plate.

Because of water vapour contamination a new channel plate will initially exhibit a large strip current even at primary potentials of only 100 volts, but this will rapidly drop to a low level on vacuum pumping and will continue to decrease slowly under low permanent voltage by removal of other contaminants by a form of electrolysis. It is therefore advisable to maintain the channel plate at a potential of the order of 100 volts in vacuum for an initial period prior to use and also when on "standby". Any instability or unusual value in the strip current is usually traceable to poor contacts or noisy operation due to contamination and/or poor vacuum, when ion feedback can cause spurious background signals and degradation of performance (12). For the Mullard channel plate used here typical values of the strip current (using a $10\text{ M}\Omega$ limiting resistor and a voltmeter with a $10\text{ M}\Omega$ input impedance) are of the order of $0.01\text{ }\mu\text{A}$ at 100 volts potential

rising linearly to $0.1\text{ }\mu\text{A}$ at 1 kilovolt.

Figure 3 shows strip current as a function of primary voltage for this channel plate as received and after conditioning for one week at a permanent potential of 100 volts.

The primary negative potential to the front face of the channel plate (rear face earthed) is supplied by batteries for low voltages (100 V), and by a stabilised E.H.T. unit for higher values. A pulsed voltage of short duration, triggered to coincide with the discharge under investigation, can also be added to a low standing voltage through a decoupling capacitor. This voltage pulse is monitored from the channel plate through a further decoupling capacitor and recorded synchronously with the discharge monitor display on an oscilloscope. The positive secondary potential of up to 10 kilovolts is applied to the front face of the scintillator from another stabilised E.H.T. unit. Figure 4 is a schematic diagram showing the essential elements of the monitoring and supply circuits as they would be used in a typical experimental arrangement.

Theoretical Gain and Sensitivity

Electron gain/voltage curves are shown in Figure 5 for electron and X-ray excitation of a

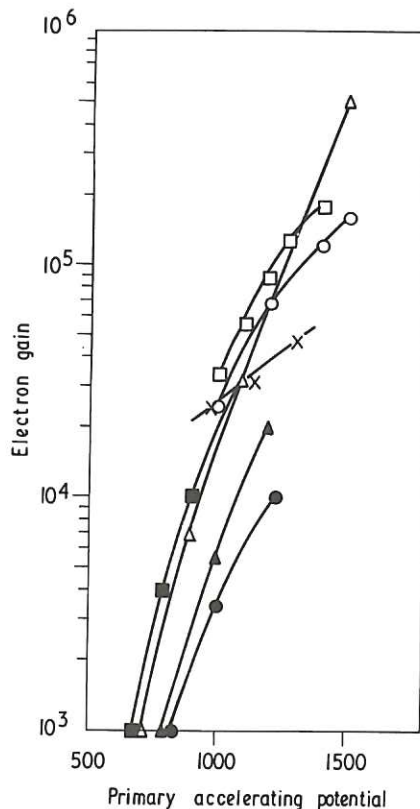


Figure 5. Electron gain as a function of accelerating potential for a variety of channel plates with a length/diameter ratio of 40. Diagram reproduced from reference (13).

variety of channel plates with the same channel length to diameter aspect ratio. This figure is reproduced from a recent comprehensive review of channel plate characteristics (13). The curve for X-ray excitation of the Mullard G40-25 type of channel plate used here indicates a gain of 2×10^4 at 1 kilovolt. The photon gain of the whole intensifier system will obviously depend on this parameter but will be modified by absorption losses and conversion efficiencies within the system. Taking all these into consideration the photon gain can be represented by the relation

$$G_{\text{phot}} = E_{\text{phot}} \cdot g \cdot T_{\text{Al}} \cdot E_{\text{phos}} \cdot T_{\text{fibre}}.$$

In this expression E_{phot} is the channel plate photon detection efficiency, which varies with wavelength and the angle of incidence of the radiation on the channels as shown in Figures 6(a) and (b). The data for these figures were

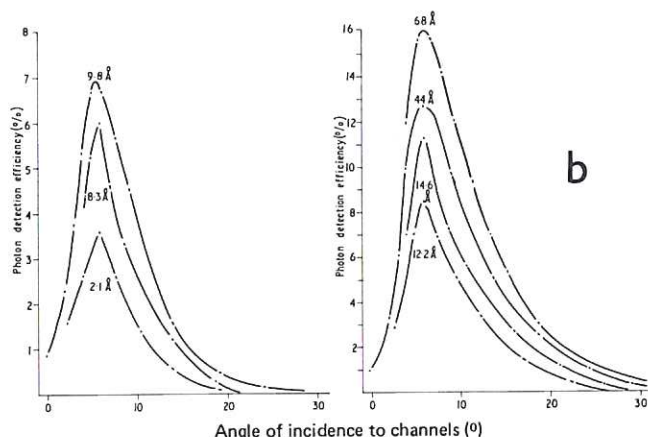
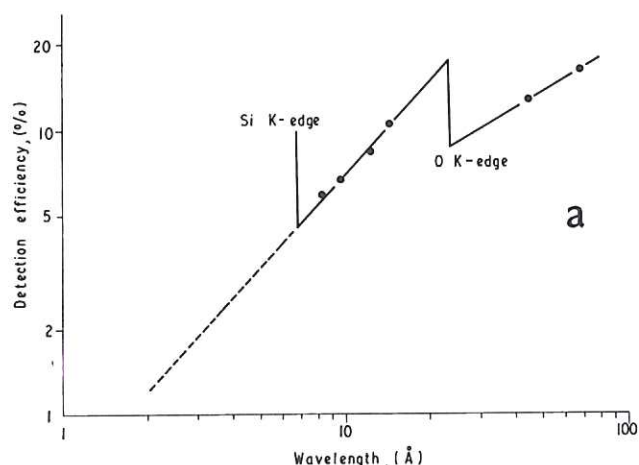


Figure 6. The efficiency of a Mullard G40-25 channel plate to X-radiation, (a) as a function of wavelength, (b) as a function of angle of incidence of the radiation on the plate. The data for these diagrams was obtained from reference (6).

obtained from reference (6). At 10 \AA and the optimum angle of incidence (7°) E_{phot} is 7%.

(Note the Mullard G40-25 channel plate is cut with the channels at 13° to the plane surface).

g is the electron gain - 2×10^4 at 1 kilovolt. T_{Al} is the number-and energy-transmission of the 250 \AA aluminium coating on the scintillator for 7 kilovolt electrons. The energy loss is very small - of the order of 100 eV. The number transmission can be calculated from an exponential decay law using Lenard's absorption coefficient (14) and is 51%.

E_{phos} is the conversion factor of the scintillator or the number of scintillator photons produced per incident electron. This is given by $N = S \cdot E / E_p$ where S is the absolute efficiency of the scintillator, E is the electron energy and E_p is the energy of the scintillator photon. Often E_p/S is specified separately as the electron energy required to produce one photon. For anthracene $S = 0.038$ and $E_p = 3 \text{ eV}$, so E_p/S is 80 eV/photon. NE 102 has 65% of the light output of anthracene so the figure here is 125 eV/photon.

T_{fibre} is the transmission of the fibre optics at the 4250 \AA wavelength of the scintillator radiation. For glass fibres 3 mm long T_{fibre} is of the order of 50%.

Thus a typical value of G would be

$$\begin{aligned} G_{\text{phot}} &= 7 \times 10^{-2} \cdot 2 \times 10^4 \cdot 5.1 \times 10^{-1} \cdot \frac{7 \times 10^3}{125} \\ &= 5 \times 10^{-1} \\ &= 2.0 \times 10^4 \end{aligned}$$

The improvement in sensitivity over direct photographic recording of the X-ray image will not however be commensurate with the photon gain because of the lower sensitivity of film to scintillator wavelengths compared with X-ray wavelengths. For a density of 0.5, exposures with a fast X-ray film are of the order of 5×10^7 photons/cm² at 10 \AA , while fast blue sensitive films require exposures of 10×10^9 photons/cm² for the same density. Thus gains in sensitivity will be approximately two orders of magnitude less than photon gains. The absolute sensitivity of such an intensifying system at a particular wavelength may be calculated from the relation

$$S = G_{\text{phot}} \cdot P$$

where P is the emulsion response factor of the recording film, usually expressed in units (density photon⁻¹ cm²). To give a density of 1.0 the exposure of Kodak Kodirex to blue light is 27.1×10^9 photons/cm² - Figure 7. The plate response factor is therefore 3.68×10^{-11} density photon⁻¹ cm² and a typical sensitivity would be

$$S = 2.0 \times 10^4 \times 3.68 \times 10^{-11}$$

$$= 7.36 \times 10^{-7} \text{ density photon}^{-1} \text{ cm}^2.$$

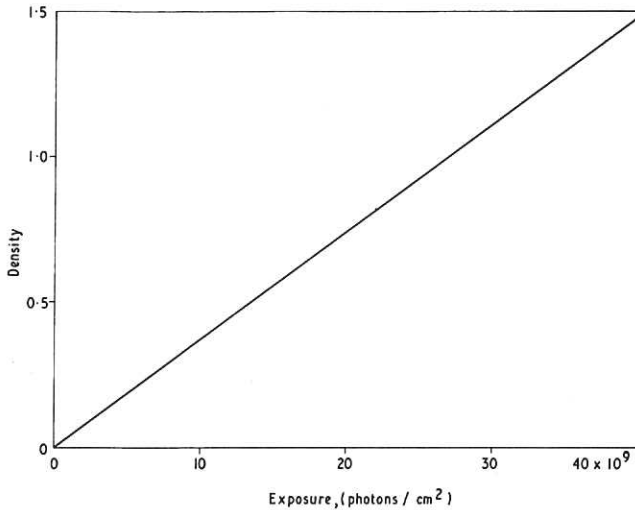


Figure 7. Absolute characteristic curve of Kodak Kodirex for blue light ($\sim 4500 \text{ \AA}$). Developed in Kodak Dx80 for 4 mins @ 20°C .

Gain Calibration and Absolute Sensitivity

Determination

The dependence of the gain on various operational parameters was first investigated in order to optimise its value. For such relative measurements, variation of density in the recording film for constant input conditions to the channel plate was used as a measure of the gain dependence since the characteristic curve of Kodirex is completely linear up to and beyond densities of 1.5 - Figure 7. Using $\text{Cu K}\alpha$ radiation from a Phillips X-ray source diffracted in 5th order from a mica crystal in the de Broglie configuration (2), a selection of fast recording films were evaluated for the highest speed with respect to the blue scintillator emission. Of those tested - Ilford Q2, Ilford FP4 (ASA 125), Kodak High Speed Recording Film (ASA 1250) and Kodak Kodirex X-ray film (ASA ~ 1000) the latter two were the most sensitive. Kodirex, although marginally slower, gave a better contrast and had the additional advantage of allowing operation in safelight conditions instead of total darkness. This film was used in all subsequent working.

No variation in gain was detected on increasing the separation between the plate and scintillator from 2 to 3 mm when the secondary potential was 5 kilovolts. This parameter does not seem to be a critical one as far as gain is concerned; so the separation required when high voltages are used can be maintained for lower voltage operation.

Figures 8 and 9 show the variation in gain,

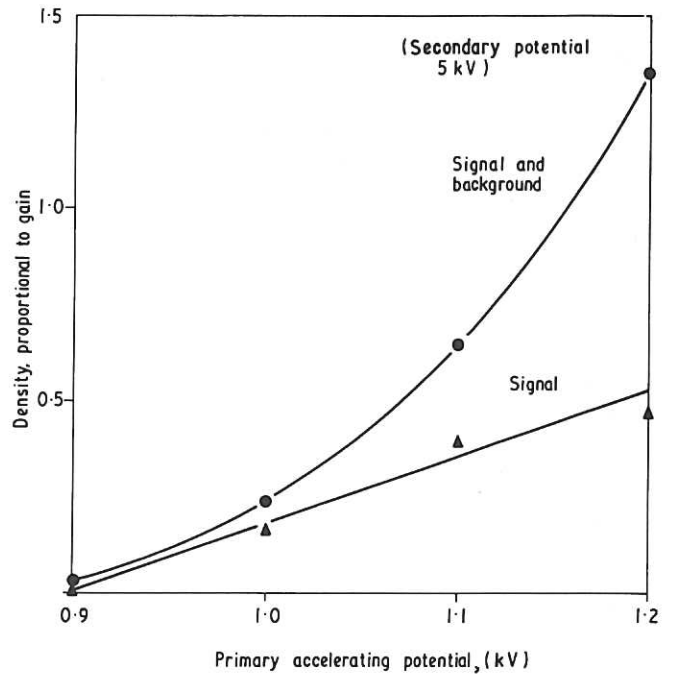


Figure 8. Variation of gain, expressed as density, with primary potential. Secondary potential 5 kilovolts.

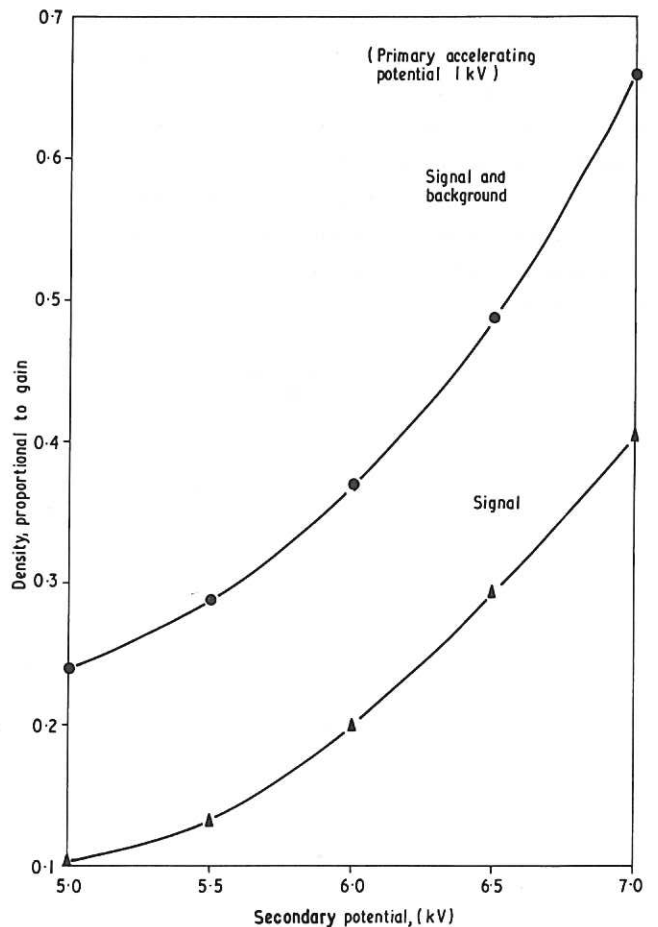


Figure 9. Variation of gain, expressed as density, with secondary potential. Primary potential 1 kilovolt.

expressed as density, with the primary and secondary potentials respectively. Increasing the primary potential linearly increases the signal gain but contrast becomes progressively

worse because background noise increases exponentially. However increasing the secondary potential shows a smooth increase of both signal and noise over the range 5-7 kilovolts. Gain is limited solely by the maximum potential that can safely be applied to the scintillator before inhomogeneities in the field strength across it cause tracking and breakdown. Optimum values for this system were therefore set at 1.0 kilovolts for the primary potential and 7.0 kilovolts for the secondary potential. The angle of incidence of the primary X-rays on the channel plate was carefully adjusted to the correct angle for maximum efficiency once a signal had been obtained.

The gain and absolute sensitivity of the intensifier were determined at three wavelengths - 1.54 \AA ($\text{CuK}\alpha$), 5.37 \AA ($\text{SiK}\alpha$) and 9.89 \AA ($\text{MgK}\alpha$) obtained from standard X-ray sources and dispersed from a curved mica crystal in the de Broglie configuration - Figure 10. The lines were first recorded directly on Kodirex film and then with the intensifier system using the optimum conditions specified above. The exposures in each case were chosen to give approximately the same density on the film with and without the intensifier. The photon gains and absolute sensitivities were evaluated from the known responses of Kodirex film to X-rays (15) and blue light, Figure 7, and from the ratio of the

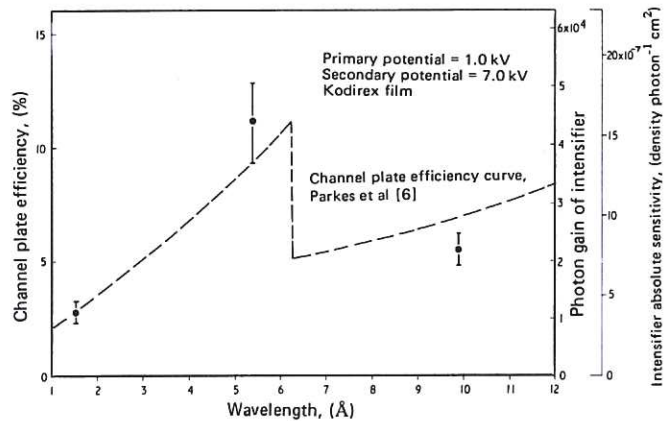


Figure 11. Photon gain and absolute sensitivity of the image intensifier as a function of wavelength compared with the channel plate efficiency. The efficiency curve is reproduced from reference (6).

exposures. Figure 11 shows the determined values and compares the wavelength dependence with the efficiency of the channel plate alone (6). The results are also tabulated in Table 1 for convenience. Typical errors are of the order of $\pm 15\%$ in both quantities, due mainly to a large uncertainty in the blue light calibration introduced by the use of an intermediate standard. The gain and sensitivity variations are obviously determined exclusively by the efficiency of the channel plate: note particularly the effect of the Si K absorption edge. The experimental values also compare favourably with the theoretically derived values of the previous section.

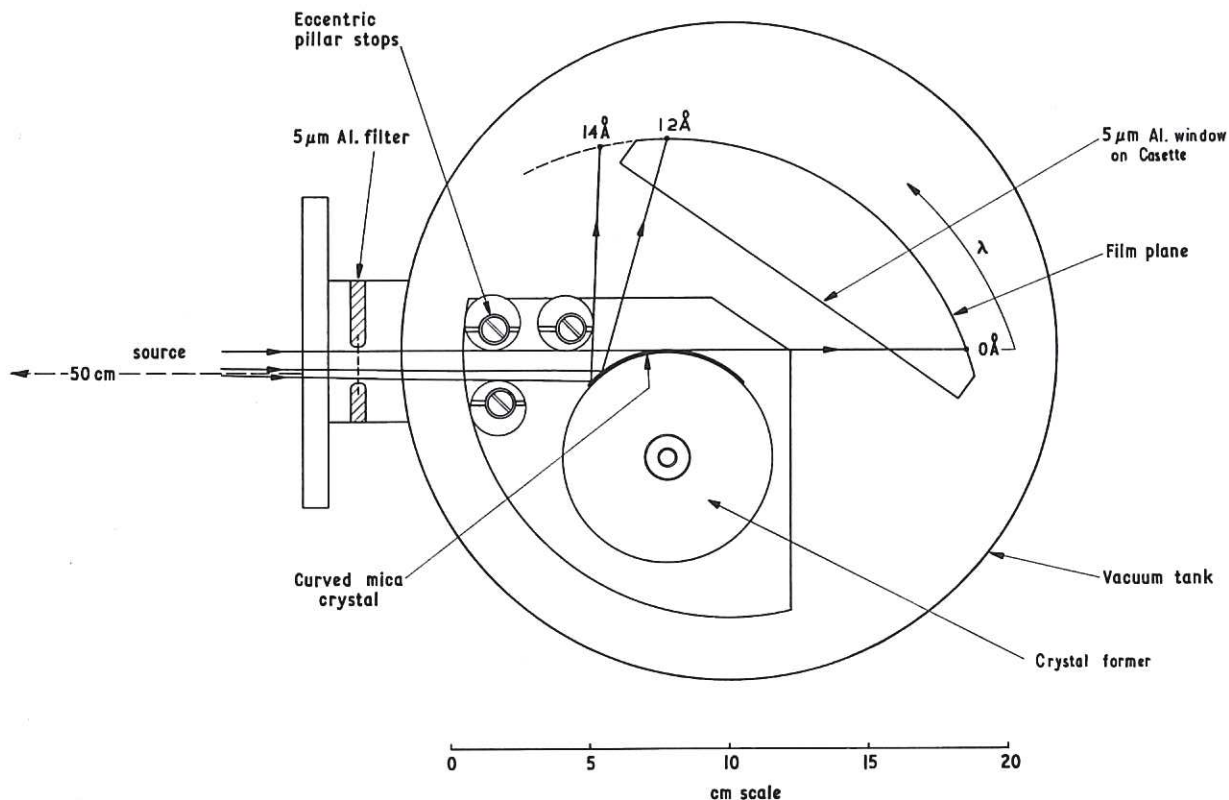


Figure 10. de Broglie Spectrometer.

Wavelength \AA	Photon Gain	Sensitivity (density. photon $^{-1}\text{cm}^2$)	Exposure for D=0.5 (pho- tons/ cm^2)
1.54 $\text{CuK}\alpha$	$(1.1 \pm 0.2) \times 10^4$	$(4.0 \pm 0.6) \times 10^{-7}$	$(12.5 \pm 1.9) \times 10^5$
5.37 $\text{S K}\alpha$	(4.4 ± 0.7)	(16.1 ± 2.4)	(3.1 ± 0.5)
9.89 $\text{MgK}\alpha$	(2.2 ± 0.3)	(7.9 ± 1.2)	(6.3 ± 1.0)

Table I. Gain and Absolute Sensitivity Determinations of Channel Plate Intensifier at Various Wavelengths.

Resolution

Resolution of detail by the intensifier depends on the pitch of the channel plate capillaries, the spreading of the electron trajectories as they leave the rear face of the channel plate and in the aluminium coating, light scattering in the scintillator and at interfaces, and on the pitch of the fibre-optic channels. Film granularity might also be a contributory factor when using extremely-fine-pitch channel plate arrays (of the order of a few microns) but can be neglected here. The effect of the fibre-optic pitch can be neglected by ensuring that it is commensurate with channel plate capillary pitch. By making the secondary potential as high as possible and keeping the spacing between the plate and scintillator small, by using very thin layers of scintillator and aluminium coating and by ensuring intimate contact of mating surfaces, degrading of the image due to the other effects can be minimised and resolution will depend predominantly on the channel capillary pitch. A thin scintillator is also advisable to discriminate against excitation by neutrons or X-rays in experimental conditions and it certainly need only be a few microns thick to stop all the entering electrons. The channel pitch of the G40-25 plate used here is $50 \mu\text{m}$, which, at a 'dispersion' of $0.02 \text{\AA}/\text{mm}$ in the de Broglie spectrometer using mica in fifth order, represents a wavelength interval of 0.001\AA .

Figure 12 illustrates the resolution of the intensifier, (b), compared with that obtained by direct photographic recording on Kodirex film, (a). The $\text{CuK}\alpha$ doublet was dispersed in 5th order, from a mica crystal in the de Broglie spectrometer. The F.W.H.M. of each of the component lines is 0.002\AA directly on film and 0.004\AA with the intensifier (covering 4 channels). This is commensurate with the separation of the pair and they are just resolved.

Plasma Diagnostics and High-Speed Shuttering

The instrument was incorporated in the de Broglie spectrometer as an alternative detector to photographic film and was used to observe and

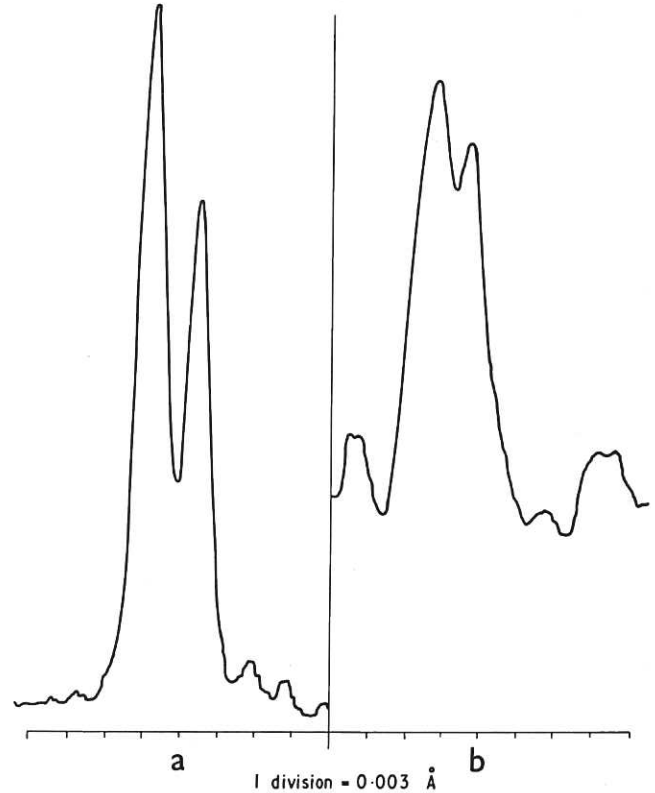


Figure 12. Microdensitometer traces of the $\text{CuK}\alpha$ doublet dispersed in 5th Order from a curved mica crystal, (a) recorded directly on Kodirex film, (b) recorded with the image intensifier.

record X-radiation dispersed from two high-density plasmas. These were the dense pinch produced in a plasma focus discharge, and the plasma produced at a solid surface by focused radiation from a high-powered laser. As an important adjunct to its rôle as a straightforward image intensifier when a standing primary potential is applied, the device was also employed as a high-speed shutter by applying the primary potential as a pulse of very short duration synchronised with the plasma discharge. In practice a pulse of 400 volts was superimposed on a standing bias of 600 volts. As gain at 600 volts is only a few percent of that at one kilovolt very little radiation reaching the multiplier outside the pulse duration will be recorded.

When observing the spectrum of highly-ionised

fluorine generated by focusing the radiation from a 1.5 GW neodymium laser onto a plane, solid 'P.T.F.E.' target, the level of F IX Ly α radiation (14.984 Å) recorded with one discharge was commensurate with that requiring 50 discharges using direct photographic recording (4), indicating a gain comparable to that determined during calibration. With a 40 nsec gating pulse the Ly α intensity was identical to that recorded with a standing bias; full amplification is therefore maintained during the gating process. The fact that the intensity ratio (0.42) of F IX Ly α to the second member of the F VIII He-like series is very similar to that (0.47) observed with photographic recording and is identical in continuous and pulsed operation shows that amplification is not a function of intensity and that this property is also maintained during gating. When the gating pulse was only partially synchronous with the plasma discharge the intensity was reduced by a factor of 8.5, while with a completely desynchronised pulse the radiation level was reduced by a factor of 90, being that recorded with the 600V standing bias. Successful recording was also obtained with a pulse of 12 nsec duration. The radiation level was 30% of that of the ungated value suggesting that the lifetime of the Ly α -emitting region was of the order of 36 nsec.

In the case of the plasma focus where the dense pinch phase has a lifetime of the order of 50-100 nsec the gain-coupled gating facility introduces the possibility of short-exposure time-resolution studies of the discharge in the X-ray region which will be complementary to laser interferometric studies performed previously (1). To assess the feasibility of such studies preliminary gating experiments were carried out on the spectrum of highly-ionised argon produced in a 27.5 kV plasma focus discharge in 2.5 torr (D₂ + 5%A), (2). Figure 13 compares exposures taken of the part of the third order curved mica spectrum containing the A XVII resonance and intercombination lines and their associated long-wavelength satellites. Trace (a) was recorded with 6 discharges directly on Kodirex film, trace (b) with 1 discharge on the ungated image intensifier and traces (c) and (d) with 5 and 2 discharges, each with a single 40 nsec gating pulse, though in both cases this coincided with the peak of the X-ray emission (1) for only one of the discharges. Sensitivity is again improved using the intensifier and intensity ratios are clearly maintained during the gating process over a dynamic range of 10. The FWHM and

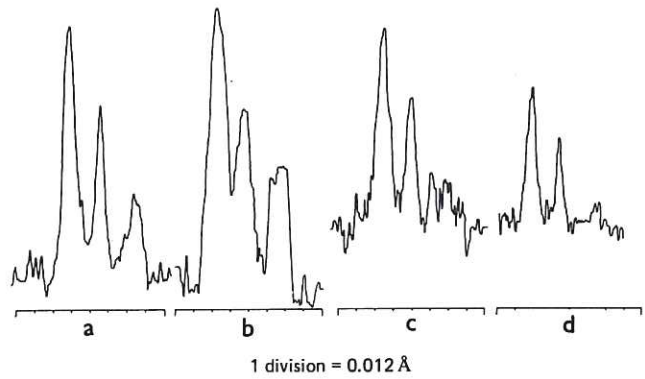


Figure 13. Microdensitometer traces of the A XVII resonance, intercombination and satellite lines dispersed in 3rd Order with a curved mica crystal from a plasma focus discharge - 27.5 kV in 2.5 torr (D₂ + 5% A).

- Trace (a) recorded directly on film (6 discharges)
- Trace (b) recorded with the ungated image intensifier (1 discharge)
- Trace (c) recorded with the image intensifier gated with a 40 nsec pulse synchronised to the peak of the X-ray emission (5 discharges though synchronised for only 1).
- Trace (d) as trace (c) (2 discharges though synchronised for only 1).

separation of the resonance and intercombination lines are 0.29 mm (0.008 Å) and 0.77 mm (0.020 Å) respectively, covered by 6 and 15 channels, so that the resolution is adequate to resolve all the features present in the film record.

Summary and Conclusions

An X-ray image intensifier based on a channel multiplier array has been constructed and absolutely calibrated in the wavelength range 1.5 - 10 Å. Sensitivity gains over direct film recording of between 20 and 110 depending on wavelength have been determined both in calibration and in the observation of crystal dispersed radiation from transient high-density plasmas. Its use as a high-speed shutter in these observations while maintaining amplification over a dynamic range of 10 has also been successfully demonstrated with exposures as short as 12 nsec. Using this gating facility the possibility of inexpensive short-exposure time-resolution studies of the plasma focus X-ray spectrum on a single-shot sequential basis has been considered and preliminary results with 40 nsec gating are presented. There is every reason to expect that exposure times as short as a few nsec can be attained, the limit being determined only by

the charging rate set by the intrinsic capacitance of the channel plate itself (of the order of 50 pf). Sensitivity could be increased by the use of P60 phosphor, for example, which has a much higher conversion efficiency for electrons than NE 102 scintillator. With careful choice of design parameters resolution depends primarily on the pitch of the channel plate capillaries - 50 μm in this case. Future developments of the system will include extending the fibre-optic transfer outside the vacuum chamber thus speeding up data readout. The coupling of an image converter camera to the device could present the readout in high-speed framing or streak modes without the need for the gating facility. Rigorous time-resolved studies of a plasma spectrum would then be possible limited only by conversion times within the system, but at much greater expense. In this instance the retention of the NE 102 scintillator in the device is imperative because of its fast decay rate compared with phosphor. In addition to diagnostics of transient plasmas applications are envisaged in medical and metallurgical fields where remote monitoring of weak X-ray fluxes is required.

Acknowledgements

We are grateful to Mr B.B. Jones and Mr.F.F. Freeman (of the Astrophysics Research Unit, SRC) for permission to use their X-ray source and for advice on its operation. We would also like to thank Dr.K.A. Pounds of Leicester University for permission to reproduce the data of Figure 6.

References

1. Peacock, N.J., Hobby, M.G. and Morgan, P.D., Proc. 4th Int. Conf. on Plasma Physics and Controlled Fusion, Madison, Vol.1, 537-51, (1971), (IAEA, Vienna).
2. Peacock, N.J., Speer, R.J. and Hobby, M.G., J. Phys. B, 2, 798-810, (1969).
3. Galanti, M. and Peacock, N.J., Proc 6th European Conf. on Controlled Fusion and Plasma Physics, Moscow, Vol.1, 427-30, (1973).
4. Peacock, N.J., Hobby, M.G., and Galanti, M., J.Phys. B, 6, L298-304, (1973).
5. Adams, J. and Manley, B.W., Phillips Tech.Rev., 28, 156-161, (1967).
6. Parkes, W., Gott, R. and Pounds, K.A., IEEE Trans. Nucl. Sci., NS17, 360-370, (1970).
7. Galanti, M., Gott, R. and Renaud, J.F., Rev. Sci. Inst., 42, 1818-1822, (1971).
8. Bettinali, L., Pecorella, F. and Rager, J-P., Rev. Sci. Inst., 42, 1834-1836, (1971).
9. Bettinali, L., Percorella, F., and Rager, J-P., to be published in Rev. Sci. Inst.
10. Hunter, W.R., and Marlow, F.E., Appl. Optics, 12, 968-971, (1973).
11. Leiber, A.J., Rev. Sci. Inst., 43, 104-108 (1973).
12. Rager, J-P., and Renaud, J.F., submitted for publication in Rev. Sci. Inst.
13. Rager, J-P., Laboratorio Gas Ionizzati, Rep. No. LGI 72/12/E, (1972)
14. Lenard, P., Handbuch d Experimentalphysik, XIV, 178, Akad Verlag, Leipzig, (1927).
15. Hobby, M.G., and Peacock, N.J., J. Phys. E, 6, 854-857, (1973).



HER MAJESTY'S STATIONERY OFFICE

Government Bookshops

49 High Holborn, London WC1V 6HB
13a Castle Street, Edinburgh EH2 3AR
41 The Hayes, Cardiff CF1 1JW
Brazenose Street, Manchester M60 8AS
Wine Street, Bristol BS1 2BQ
258 Broad Street, Birmingham B1 2HE
80 Chichester Street, Belfast BT1 4JY

*Government publications are also available
through booksellers*